



Published in final edited form as:

*Biomacromolecules*. 2012 February 13; 13(2): 342–349. doi:10.1021/bm201763n.

## Promoting Nerve Cell Functions on Hydrogels Grafted with Poly(L-lysine)

Lei Cai<sup>†</sup>, Jie Lu<sup>§</sup>, Volney Sheen<sup>§</sup>, and Shanfeng Wang<sup>†,‡,\*</sup>

<sup>†</sup>Department of Materials Science and Engineering, The University of Tennessee, Knoxville, TN 37996

<sup>‡</sup>Biosciences Division, Oak Ridge National Laboratory, Oak Ridge, TN 37831

<sup>§</sup>Department of Neurology, Beth Israel Deaconess Medical Center, Harvard Medical School, Boston, MA 02115

### Abstract

We present a novel photo-polymerizable poly(L-lysine) (PLL) and use it to modify polyethylene glycol diacrylate (PEGDA) hydrogels for creating a better, permissive nerve cell niche. Compared with their neutral counterparts, these PLL-grafted hydrogels greatly enhance pheochromocytoma (PC12) cell survival in encapsulation, proliferation, and neurite growth, and also promote neural progenitor cell proliferation and differentiation capacity, represented by percentages of both differentiated neurons and astrocytes. The role of efficiently controlled substrate stiffness in regulating nerve cell behavior is also investigated and a polymerizable cationic small molecule, [2-(methacryloyloxy)ethyl]-trimethylammonium chloride (MTAC), is used to compare with this newly developed PLL. The results indicate that these PLL-grafted hydrogels are promising biomaterials for nerve repair and regeneration.

### Keywords

Polyethylene glycol diacrylate (PEGDA); Photo-polymerizable poly(L-lysine) (PLL); Positive charges; Hydrogel; Neural progenitor cell differentiation

### Introduction

Functional nerve regeneration is a complex biological process which requires precisely controlled spatiotemporal interplay between regenerative cells and guidance materials.<sup>1-4</sup> To achieve optimal performance, nerve conduits need integration of different materials that can promote nerve cell functions. For example, biodegradable hydrophobic poly( $\epsilon$ -caprolactone) (PCL) networks<sup>5-9</sup> and hydrogels based on polyethylene glycol (PEG)<sup>1-4</sup> have been used to fabricate nerve conduits and luminal fillers, respectively. Surface stiffness and chemistry of polymer networks can be readily tailored by varying the precursor molecular weight and incorporating biofunctional molecules, respectively.<sup>3,4,10-12</sup>

Substrate stiffness is critical in determining cell behavior.<sup>12-14</sup> Pheochromocytoma (PC12) cells exhibit greater neurite extension on softer PEG-based hydrogels<sup>10</sup> and mesenchymal

\*To whom correspondence should be addressed. swang16@utk.edu. Tel: 1-865-974-7809; Fax: 1-865-974-4115. .

**Supporting Information Available:** Storage modulus  $G'$ , loss modulus  $G''$ , and viscosity  $\eta$  as functions of frequency for neutral, MTAC-grafted, and PLL-grafted PEGDA hydrogels at 37 °C. This material is available free of charge via the Internet at <http://pubs.acs.org>.

stem cell (MSC) differentiation can be directed by the substrate elasticity comparable to its native tissue.<sup>15</sup> Neural progenitor cell (NPC) proliferation rate and differentiated lineage can also be regulated by substrate stiffness.<sup>16-20</sup> As important chemical factors, coating of polymer substrates with integrin receptors such as Arg-Gly-Asp (or RGD) peptide and/or charged molecules can control cell behavior.<sup>21-27</sup> Because PEG is inherently inert to protein adsorption and cellular affinity, chemical modification by immobilizing functional moieties such as acrylated RGD on the surface has been applied to improve the cytocompatibility and bioactivity of PEG-based hydrogels.<sup>21-23</sup> Positive charges are believed to participate in cellular activities and functions such as attachment, proliferation, differentiation, and neurite outgrowth.<sup>24-30</sup> Through the electrostatic interactions with the anion sites of cytoplasmic membrane, cationic poly(L-lysine) (PLL) can provide both cell binding sites and positive charges to promote cell functions.<sup>27-30</sup> With the exception of functionalizing the amino groups of PLL,<sup>27,28</sup> no efficient way exists to covalently incorporate PLL chains into hydrogel. The functionalization of these groups,<sup>27,28</sup> however, leads to a loss of positive charges because of less dissociation of secondary amine groups.

Here we present a novel photo-polymerizable PLL and use it to modify PEG diacrylate (PEGDA) hydrogels for creating a better, permissive nerve cell niche. Initiated by allylamine, efficient ring-opening polymerization of carbobenzyloxy-L-lysine-*N*-carboxyanhydride (Z-L-Lys NCA) yielded PLL end-capped with a reactive allyl group, which can be further covalently linked into PEGDA networks via photo-crosslinking (Figure 1). PEGDA was synthesized using facile condensation between PEG and acryloyl chloride in the presence of potassium carbonate ( $K_2CO_3$ ) as the proton scavenger, replacing widely used triethylamine (TEA) which could form a colored complex with acryloyl chloride.<sup>7,31,32</sup> By varying the molecular weight of the PEG precursor, hydrogels made from PEGDA have different crosslinking densities and therefore different mechanical properties. Through photo-crosslinking, PEGDA hydrogels were grafted with a low concentration of 1 wt.% PLL in aqueous solution to provide cell binding sites and positive charges while the mechanical properties remained intact. To compare with this photo-polymerizable PLL and demonstrate the sole role of positive charges, [2-(methacryloyloxy)ethyl]-trimethylammonium chloride (MTAC) with an end-capped carbon-carbon double-bond, a widely used cationic small molecule to modify neutral hydrogels,<sup>26,33</sup> was also grafted into PEGDA hydrogel (Figure 1). Using these neutral and positively charged PEGDA hydrogels, we have evaluated attachment, proliferation, encapsulation, and differentiation of rat PC12 cells and mouse NPCs. Results from these studies can help us achieve better understanding on how to optimize material properties for promoting nerve cell functions and scaffold performance.

## Experimental Section

### Synthesis of PEGDA

All chemicals were purchased from Sigma-Aldrich (Milwaukee, WI) unless otherwise noted. PEGs with nominal molecular weights of 1k, 3k, and 10k  $g\ mol^{-1}$  were dried overnight in a vacuum oven at 50 °C. Determined using the Gel Permeation Chromatographic (GPC) system described later, these PEGs had number-average molecular weights ( $M_n$ s) of 1300, 5240, 14000  $g\ mol^{-1}$ , weight-average molecular weights ( $M_w$ s) of 1410, 5400, 14500  $g\ mol^{-1}$ , and polydispersity values of 1.08, 1.03, 1.04, respectively. Acryloyl chloride was used as received. Methylene chloride was dried and distilled over calcium hydride. Ground  $K_2CO_3$  was dried at 100 °C overnight and then cooled down in vacuum prior to the reaction. PEG (50 g) was dissolved in methylene chloride (100 mL) in a 500 mL three-neck flask along with  $K_2CO_3$  in a molar ratio of 1:3. With the same molar amount as  $K_2CO_3$ , acryloyl chloride was dissolved in methylene chloride (1:10 v/v) and added dropwise to the slurry mixture. The reaction was maintained at room temperature

under nitrogen for 24 h. The mixture was then filtered to remove the solids (KCl,  $\text{KHCO}_3$ , and unreacted  $\text{K}_2\text{CO}_3$ ), precipitated twice in diethyl ether and dried completely in vacuum.

### Synthesis of PLL

$\epsilon$ -carbobenzyloxy-L-lysine (*Z*-L-Lys, 8 g, 28.6 mmol) was dissolved in anhydrous THF (200 mL) in a 500 mL three-neck flask and stirred at 50 °C. Triphosgene (2.83 g, 9.55 mmol) in anhydrous THF (50 mL) was added dropwise to the flask in a period of 1 h. The reaction was continued for 2 h under nitrogen flux. The solution was filtered, concentrated, and precipitated twice in anhydrous hexane (300 mL). The recrystallized *Z*-L-Lys-*N*-carboxyanhydride (*Z*-L-Lys NCA) was dried completely in vacuum and the yield was ~90%.<sup>33</sup> Polymerization was conducted in a Schlenk tube under nitrogen. The *Z*-L-Lys NCA (10 mmol) was dissolved in anhydrous dimethylformamide (DMF, 30 mL) with anhydrous allylamine (0.2 mmol) as an initiator. The reaction was proceeded at 40 °C for 3 days until all the monomer was consumed. Then DMF was removed in vacuum. The crude polymer (2 g) was dissolved in trifluoroacetic acid (10 mL) and chloroform was then added until a slight cloudiness was observed. A 33 wt.% hydrobromic acid solution in glacial acetic acid (20 mL) was added to the polymer solution and the mixture was slowly stirred for 1 h at room temperature. The mixture was then precipitated, filtered, and washed twice in cold diethyl ether and the obtained PLL was dried completely in vacuum.

### Structural characterization

Polymer molecular weights were measured on an EcoSEC Gel Permeation Chromatographic (GPC) system (Tosoh Bioscience LLC, Montgomeryville, PA) with tetrahydrofuran (THF) as the eluent. The chemical structures of PEGDA and photo-polymerizable PLL were confirmed by  $^1\text{H}$  NMR and IR (Figure 2).  $^1\text{H}$  NMR spectra were acquired on a Varian Mercury 300 spectrometer (300 MHz) using  $\text{CDCl}_3$  containing tetramethylsilane (TMS) as the solvent. IR spectra were obtained on a Perkin Elmer Spectrum Spotlight 300 spectrometer with Diamond Attenuated Total Reflectance. NMR for PEGDA (Figure 2a):  $\delta$  = 6.5, 6.2, 5.9 (6H,  $\text{H}_2\text{C}=\text{CH}-$ ), 3.6 (PEG chain protons). IR for PEGDA (Figure 2b): 2883  $\text{cm}^{-1}$  ( $-\text{CH}_2-$ ), 1724  $\text{cm}^{-1}$  ( $-\text{C}=\text{O}$ ), 1635  $\text{cm}^{-1}$  ( $\text{H}_2\text{C}=\text{CH}-$ ). NMR for photo-polymerizable PLL (Figure 2c):  $\delta$  = 5.3 (3H,  $\text{H}_2\text{C}=\text{CH}-$ ), 3.2, 1.8, 1.5, 1.2 (t, 2H,  $-\text{CH}_2-$ ), 4.3 (t, 1H,  $-\text{CH}-$ ), 6.8 (s, 1H,  $-\text{NH}$ ). IR for photo-polymerizable PLL (Figure 2d): 3389  $\text{cm}^{-1}$  ( $-\text{NH}_2$  asymmetric stretching), 3243  $\text{cm}^{-1}$  (amide II) and 3033  $\text{cm}^{-1}$  (N-H stretching vibration), 1650, 1539, 1392  $\text{cm}^{-1}$  (amide I, II, III bands, respectively). The carbon-carbon double-bond peak in the IR spectra was buried in the strong signals from amide bands.

### Hydrogel preparation and characterization

To achieve an equal feed amount of positive charges, 1 wt.% (3 mM) photo-polymerizable PLL or 72 mM MTAC was dissolved in deionized water with 30 wt.% PEGDA and 0.05 wt.% photo-initiator, 4-(2-hydroxyethoxy)phenyl-(2-hydroxy-2-propyl)ketone (Irgacure 2959, Ciba Specialty Chemicals, Tarrytown, NY) as the precursor solution. Photo-crosslinking of the precursor solution was initiated with UV light ( $\lambda = 365$  nm) from a high-intensity (4800  $\mu\text{W}/\text{cm}^2$ ) long-wave UV lamp (SB-100P, Spectroline) for 10 min. By measuring the weights of the original ( $W_0$ ), dry ( $W_d$ ), and fully swollen ( $W_s$ ) polymer disks as described by us earlier,<sup>7</sup> their swelling ratios and gel fractions were calculated using the equations of  $(W_s - W_d)/W_d$  and  $W_d/W_0 \times 100\%$ , respectively. Linear viscoelastic properties of crosslinked PEG-based hydrogels were measured using a strain-controlled rheometer (RDS-2, Rheometric Scientific) donated by Patel Scientific and the same procedure described in our previous report.<sup>7</sup> The molar fractions of C, N, and O in the total amount of these three atoms on the completely dried disk surfaces were measured using Energy Dispersive Spectroscopy (EDS, S-3500, Hitachi Instruments Inc.) at 20 kV. Zeta-potential measurements were performed on a Delsa™ Nano C Zeta Potential Analyzer (Beckman Coulter, Inc., Brea, CA)

using homogenized hydrogel particles (~1  $\mu\text{m}$ , diameter) in 4-(2-hydroxyethyl)piperazine-1-ethanesulfonic acid (HEPES) sodium salt buffer solution (HEPES  $5 \times 10^{-3}$  M,  $\text{NaHCO}_3$   $1.55 \times 10^{-2}$  M,  $\text{NaCl}$  0.14 M,  $\text{pH} = 7.4$ ).

### In vitro PC12 cell studies

Rat PC12 cells (ATCC, Manassas, VA) were cultured in a growth medium containing F-12K Media (Gibco, Grand Island, NY), 15% horse serum, 5% fetal bovine serum (FBS, Gibco) and 1% penicillin/streptomycin (Gibco) in an incubator with 5%  $\text{CO}_2$  and 95% relative humidity at 37  $^\circ\text{C}$ . All hydrogels were cut into disks (~2.5 mm  $\times$  ~1.0 mm, diameter  $\times$  thickness), sterilized in 70% alcohol solution overnight, dried completely in vacuum, and rinsed adequately in phosphate buffered saline (PBS). PC12 cells were seeded onto the sterile hydrogel disks and empty wells as a control group in a 48-well tissue culture polystyrene (TCPS) plate at a density of ~15,000 cells/ $\text{cm}^2$  for 12 h, 1, 4, and 7 days. The attached cells were trypsinized and cell numbers were counted using a hemacytometer and normalized to the TCPS control group. Cell number was also determined from at least seven phase-contrast images and averaged. Attached cells were fixed in 4% paraformaldehyde (PFA) solution at room temperature for 10 min. Phase-contrast microscopic images of attached PC12 cells were taken using an Axiovert 25 light microscope and an AxioCam ICm1 camera (Carl Zeiss, Germany). PC12 neurites were induced in a growth medium supplemented with 50 ng  $\text{mL}^{-1}$  NGF for 7 days. Fluorescent images were taken on PC12 neurites stained using rhodamine-phalloidin (RP, Cytoskeleton Inc., Denver, CO). Neurite length, number of neurites per cell, and percentage of differentiation (percentage of cells bearing neurites in entire attached cells) were quantified over more than 10 images and 100 non-overlapping cells for each hydrogel substrate. Only neurites longer than the diameter of original, round PC12 cells (ca. 10  $\mu\text{m}$ ) were considered as positive neurite extension and cells with at least one neurite longer than 10  $\mu\text{m}$  were counted as neurite-bearing cells. For encapsulation, PC12 cells were re-suspended at a density of ~200,000 cells/ $\text{mL}$  in the precursor solution and crosslinked under UV light for 10 min. Hydrogels were then immersed in cell culture media for 1 or 7 days. Cell viability was tested using LIVE/DEAD<sup>®</sup> Viability/Cytotoxicity kit (Invitrogen, Carlsbad, CA). Live cells were stained green and dead cells were stained red in separate fluorescence images. Cell viability was determined by the number of live cells divided by the total number of stained cells. At least 500 cells were counted for each sample.

### In vitro NPC cell studies

NPCs from E14 mouse cortex were cultured using serum-free growth media containing DMEM/F12 media (Invitrogen) with 2% StemPro neural supplement (Invitrogen), 20 ng  $\text{mL}^{-1}$  basic fibroblastic growth factor (bFGF, Invitrogen), 20 ng  $\text{mL}^{-1}$  epidermal growth factor (EGF recombinant human, Invitrogen), 1% GlutaMAX (Invitrogen), and 1% penicillin/streptomycin. NPC cell attachment and proliferation were performed and analyzed using the same procedure for PC12 cells. For NPC differentiation, the growth medium was removed after cells attached onto the substrates and replaced with a differentiation medium containing DMEM/F12, 1% FBS, 1  $\mu\text{M}$  all-*trans*-retinoic acid, and 1% GlutaMAX. Cells were cultured in the differentiation media for additional 7 days. Differentiated cells were fixed and then blocked with PBS containing 0.3% Triton X-100 and 1% bovine serum albumin (BSA) at room temperature for 30 min. After blocking, cells were incubated with a diluted primary antibody including mouse monoclonal anti- $\beta$ -tubulin III (1:500) for neurons or mouse monoclonal anti-glial fibrillary acidic protein (GFAP, 1:500) for astrocytes at 37  $^\circ\text{C}$  for 1 h and then at 4  $^\circ\text{C}$  overnight. After washing using PBS containing 1% BSA for three times, cells were stained with a secondary antibody of goat anti-mouse IgG-FITC (1:100) at 37  $^\circ\text{C}$  in the dark for 2 h and then washed with PBS for three times. Finally cell nuclei were counter-stained with 4',6-diamidino-2-phenylindole (DAPI) at room

temperature for photographing. Differentiation in terms of positive antibody expression was quantified by counting the number of cells that expressed the marker divided by the total number of cells identified by DAPI staining.<sup>19</sup> At least seven images were analyzed and averaged.

### Statistical analysis

All statistical computations were performed by analysis of variance (ANOVA) followed by Tukey post-test as needed. The values were considered significantly different if the *p*-value was less than 0.05.

## Results and Discussion

Three PEGDAs used here, PEGDA1k, 3k, and 10k, were named after the nominal molecular weights of their PEG precursors and had  $M_n$ s of 1450, 5450, 14500 g mol<sup>-1</sup>,  $M_w$ s of 1560, 5640, 15300 g mol<sup>-1</sup>, and polydispersity values of 1.08, 1.03, 1.06, respectively. Photopolymerizable PLL had  $M_n$  of 3060 g mol<sup>-1</sup>,  $M_w$  of 3750 g mol<sup>-1</sup>, and polydispersity of 1.23. Their chemical structures were confirmed by use of NMR and IR spectra (Figure 2), as described in Experimental section. To prepare hydrogels with high gel fractions (67-78%, Table 1) and smooth surfaces after the soluble fraction was removed, a PEGDA concentration of 30 wt.% in deionized water was used. The swelling ratio of the PEGDA network (Table 1) increased with the molecular weight of PEG precursor because the crosslinking density decreased. Determined on a strain-controlled rheometer at 37 °C, the storage modulus  $G'$  and loss modulus  $G''$  curves of all the PEGDA hydrogels were characteristic of perfect polymer networks because  $G'$  was independent of frequency and always greater than  $G''$  (Figure S1). The shear modulus ( $G$ ) of the hydrogel, i.e., the average value of  $G'$  in the tested frequency range, almost did not change after adding MTAC or PLL while it decreased by factors of 3.2 and 23 when PEGDA changed from 1k to 3k and 10k, respectively (Table 1).

Both MTAC- and PLL-grafted hydrogels were positively charged from the dissociated amino groups. Their charge densities were measured using a zeta-potential analyzer at pH 7.4 (Table 1). The molar composition of grafted MTAC or PLL in the network, estimated from the molar fraction of N atoms, was always lower than the feed composition. For MTAC, the grafting ratio calculated by dividing the measured composition by the feed composition decreased from 91% to 80% and 74% when PEGDA changed from 1k to 3k and 10k, respectively. Because the double bond, i.e., the allyl group in longer PLL was less reactive than that in MTAC, the corresponding grafting ratios were even lower: 70%, 55%, and 48%. Consequently, PLL-grafted hydrogels had almost half lower zeta potentials than MTAC-grafted hydrogels and the zeta potential decreased slightly when PEGDA was longer in both series of hydrogels. When the feed composition of PLL was increased from 1 wt.% (Table 1) to 3 wt.%, the zeta-potential value ( $9.11 \pm 0.3$  mV) of the PLL-grafted PEG10k hydrogel was close to those of the MTAC-grafted hydrogels used here (7.4-8.8 mV).

To examine the influence of anchorage polypeptide and positive charges on cell survival in three-dimensional (3D) matrices, PC12 cells were encapsulated in the hydrogels for 1 and 7 days. Calculated from the LIVE/DEAD staining shown in Figure 3a,b, cell viability (Figure 3c) was lower at longer time periods for all the hydrogels. The highest cell viability was observed in the softest PEGDA10k hydrogel because a looser mesh not only supplied a more favorable mechanical environment, but also and more importantly could allow for more cell motion and communication and facilitate better diffusion of nutrients.<sup>12</sup> Compared with the neutral hydrogels, cell viability at day 7 was increased in MTAC-grafted hydrogels and even more so in PLL-grafted hydrogels. The viability of PC12 cells encapsulated in PLL-grafted PEGDA10k hydrogel was  $97 \pm 1\%$  at day 1 and  $93 \pm 2\%$  at day 7, significantly



higher than the day 1 values of  $88 \pm 4\%$  in neutral PEGDA10k hydrogel and  $74 \pm 6\%$  in PEGDA1k hydrogel. The results confirmed that anchorage sites and positive charges from tethered PLL chains were advantageous for cell survival in encapsulation.<sup>22</sup>

PC12 cells cultured for 7 days on the hydrogels are shown in the phase-contrast microscopic images in Figure 4a. Without exposure to nerve growth factor (NGF), PC12 cells on all the hydrogels remained rounded and did not spread. Unlike Schwann cell precursor (SpL201) cells with the glial nature, which prefer stiffer substrates,<sup>5-8</sup> PC12 cells in this study always favored softer substrates such as the PEGDA10k hydrogel by demonstrating higher attachment and faster proliferation than the PEGDA1k hydrogel (Figure 4b,c). Pure PEGDA hydrogels could not efficiently support attachment and proliferation of PC12 cells because of low protein adsorption on the hydrated layer.<sup>10,14</sup> Incorporation of MTAC or PLL significantly increased the percentage of attached cells to close to the control group on TCPS at 12 h post-seeding. Further, they could migrate and proliferate much faster with larger cell colonies on softer and positively charged hydrogels (Figure 4c).

NGF-induced differentiation of PC12 cells was also enhanced on MTAC- and PLL-grafted hydrogels. PC12 cell soma and neurites stained with RP are shown in Figure 5a. No neurites could be found on neutral PEGDA1k hydrogels, although some neurites could grow on softer PEGDA10k hydrogel substrates. PC12 neurite extension was significantly enhanced when positively charges were grafted in the hydrogels. As indicated from the analysis in Figure 5b, longer neurite length, higher percentage of differentiation, and more neurites per cell were found on the PLL-grafted hydrogels than on MTAC-grafted hydrogels, although the latter had higher zeta-potentials. These results indicated the integrative roles of both cell adhesive ligands and positive charges in fostering PC12 cell differentiation. These results agreed with previous reports that PC12 or Dorsal Root Ganglion (DRG) neurites could extend best on the softest PEGDA hydrogels with immobilized RGD ligands<sup>10</sup> and substrates grafted with positive charges.<sup>26</sup> The effect of positive charges on neurite extension may be attributed to protein conformation changes, enhancement of protein synthesis, and redistribution of cell-membrane growth factors and adhesion ligands.<sup>35</sup>

We further characterized the bioactivity of the hydrogels using NPCs, which bear multipotency and the ability of self-renewal.<sup>16-19</sup> In serum-free culture media, NPC neurospheres could migrate out or form a network between remote neurospheres, allowing for a more precise investigation of cell responses to surface charges and peptides without interference from serum proteins.<sup>29</sup> As shown in the fluorescent images in Figure 6a, NPC neurospheres were observed by staining nuclei with DAPI. Similar to the roles of substrate stiffness in regulating PC12 cell behaviors discussed earlier, NPCs also showed enhanced attachment, faster proliferation, and formed larger neurospheres on softer hydrogels of PEGDA10k than PEGDA 1k (Figure 6b,c). NPC growth rate was reported to maximize on hydrogels with a brain-tissue-like stiffness of  $\sim 3.5$  kPa,<sup>16,19</sup> which was elastic modulus ( $E$ ) and can be converted to  $\sim 1.2$  kPa for  $G$  based on the equation of  $E = 3G$ .<sup>5,19</sup> In this study, NPCs could respond to higher  $G$  values of 10-250 kPa, a more suitable range for material handling. The mechanical factor in cell-material interactions could be understood using pathways related to cell mechanotransduction and integrin-mediated focal adhesion.<sup>13,16,19</sup> More and larger neurospheres were also observed on PLL or MTAC-grafted hydrogels bearing positive charges. The proliferation index of NPCs, calculated by dividing the cell number at day 7 by the attached cell number at 4 h, increased from  $3.3 \pm 0.5$  to  $3.6 \pm 0.4$  when PEGDA1k hydrogel was grafted with MTAC. The index was further increased to  $4.1 \pm 0.5$  and  $6.2 \pm 0.6$  for PLL-grafted hydrogels of PEGDA1k and 10k, respectively. It has been hypothesized that ion channels such as voltage-gated calcium influx may be altered when cells interact with positively charged surfaces.<sup>26,36</sup> Interactions between membrane receptors and proteins may be changed as well by electrical stimulation.<sup>35</sup> These events may

facilitate cell adhesion and proliferation, although the mechanism is still under investigation. The benefit from grafted PLL by attracting negative charges on the cell membrane and providing cell anchoring sites was evident and best exhibited in the early stage of cell adhesion and at day 1, when NPCs could directly interact with the substrate before forming large colonies.<sup>16</sup>

To investigate the potential of NPC performance for central nervous system recovery, we used a differentiation medium for directing NPCs into two major neural lineages: neurons and astrocytes.<sup>19</sup> Different from mechanical modulation of NPC attachment and proliferation, the percentage of differentiated NPCs, defined by dividing the number of both neurons and astrocytes by the total cell number, did not vary much among different neutral or MTAC-grafted hydrogels, as shown in Figure 7a,b. PLL-grafted hydrogels however did show increased level of differentiation with decreasing the stiffness. In contrast, positive charges could significantly improve the extent of NPC differentiation. For the same PEGDA, the percentages of both neurons and astrocytes were significantly increased on MTAC-grafted hydrogel and even more on PLL-grafted hydrogel. Previous studies also indicated the potential for PLL to induce higher efficiency for neural tissue differentiation of embryonic brain cells via the interactions between PLL polycations and cell surfaces.<sup>30</sup> Besides this non-receptor mediated mechanism, enhanced survival rates of both lineages by PLL positive charges could also promote NPC differentiation.

We also studied the effect of the PLL feed composition in the grafted hydrogels on NPC behavior and found that NPC attachment increased by a factor of 1.4 times and NPC proliferation and differentiation could also be promoted continuously from the feed composition of 1 wt.% to 3 wt.%, at which the zeta-potential value was similar to those of the MTAC-grafted hydrogels, as mentioned earlier. Neurite outgrowth from NPCs was also observed when they were seeded at a lower density of ~5,000 cells/cm<sup>2</sup>. Beyond the scope of this study, detailed information on this composition effect will be reported with gene expression analysis by us in a subsequent paper. For both PC12 cells and NPCs, the results presented in this report were sufficient to indicate that the photo-polymerizable PLL was superior to MTAC because a much lower amount of PLL in grafted hydrogel, indicated by the lower charge density, could generate greater promotion.

Both substrate stiffness and charged ligands affected differentiation capacity of NPCs, as indicated in Figure 7a,c. When the hydrogel became softer, more neurons and fewer astrocytes were observed, although the total number of differentiated NPCs remained invariant. This trend for NPC differentiation on PEGDA hydrogels found in this study was consistent with the findings on other hydrogel systems made from methacrylamide chitosan,<sup>16</sup> alginate,<sup>17</sup> interpenetrating networks of polyacrylamide (PAM) and PEG,<sup>19</sup> and hyaluronic acid.<sup>20</sup> Though there lacks a regulatory mechanism to elucidate the lineage commitment of NPCs, the trend can be attributed to either an instructive role of stiffness, which favors differentiation through a specific pathway, or a selective role of differentially preferred survival rates in response to stiffness after NPCs differentiated into two lineages to a similar extent.<sup>19</sup> A previous report suggested this selective survival by showing more increased neurons compared to astrocytes when mixed rat embryonic cortical dissociations were cultured on soft PAM hydrogels.<sup>37</sup>

PEGDA hydrogels functionalized with PLL have great potential in fabricating nerve conduits, luminal fillers, or NPC carriers to guide functional recovery of nerve cells and axonal growth. In future studies, we will explore targeted 3D nerve cell responses both *in vitro* and *in vivo* using these hydrogel niches and investigate the concentration dependence of PLL. Dynamic tuning of PLL or spatiotemporally controlled cleavable PLL segments can retain and release favorable factors for promoting nerve cell functions. This photo-

crosslinkable PLL can be used to modify many other polymers and the tethered chains provide sites for further chemical modifications to assist regeneration of the nervous system.

## Conclusions

A novel photo-polymerizable PLL with one end-capped allyl group has been synthesized for incorporating both cell integrin anchoring sites and positive charges into PEGDA hydrogels. PEGDA hydrogels modified with 3 mM PLL offered tunable microenvironmental cues. Compared with positively charged small molecular MATC, PLL could more greatly promote PC12 cell attachment, proliferation, neurite outgrowth, and viability in encapsulation, as well as NPC attachment and proliferation. Increased neuronogenesis at the expense of astrocyte production was observed following induction of NPC differentiation on the softer PEGDA hydrogels. Both differentiation lineages could be enhanced by tethered PLL chains. The present results demonstrated that covalent immobilization of PLL in PEGDA hydrogels are promising injectable materials for nerve repair and regeneration.

## Supplementary Material

Refer to Web version on PubMed Central for supplementary material.

## Acknowledgments

This work was supported by the start-up fund of the University of Tennessee and National Science Foundation (DMR-11-06142) (to SW). We thank Minfeng Jin and Dr. Federico M. Harte for assistance with zeta-potential measurement.

## References

- (1). Schmidt CE, Leach JB. *Annu. Rev. Biomed. Eng.* 2003; 5:293. [PubMed: 14527315]
- (2). Madigan NN, McMahon S, O'Brien T, Yaszemski MJ, Windebank AJ. *Respir. Physiol. Neurobiol.* 2009; 169:183. [PubMed: 19737633]
- (3). Wang, S.; Cai, L.; Kulshrestha, AS.; Mahapatro, A.; Henderson, LA. *Biomaterials*. Vol. 1054. American Chemical Society; Washington, DC: 2010. p. 43-63.
- (4). Wang S, Cai L. *Int. J. Polym. Sci.* 2010:138686.
- (5). Wang S, Kempen DH, Simha NK, Lewis JL, Windebank AJ, Yaszemski MJ, Lu L. *Biomacromolecules*. 2008; 9:1229. [PubMed: 18307311]
- (6). Wang S, Yaszemski MJ, Knight AM, Gruetzmacher JA, Windebank AJ, Lu L. *Acta Biomater.* 2009; 5:1531. [PubMed: 19171506]
- (7). Cai L, Wang S. *Polymer*. 2010; 51:164.
- (8). Cai L, Wang S. *Biomaterials*. 2010; 31:7423. [PubMed: 20663551]
- (9). Cai L, Lu J, Sheen V, Wang S. *Biomacromolecules*. 2012 Doi: 10.1021/bm201372u.
- (10). Gunn JW, Turner SD, Mann BK. *J. Biomed. Mater. Res.* 2005; 72A:91.
- (11). Marklein RA, Burdick JA. *Adv. Mater.* 2010; 22:175. [PubMed: 20217683]
- (12). Nemir S, West JL. *Annu. Biomed. Eng.* 2009; 38:2.
- (13). Discher DE, Janmey P, Wang YL. *Science*. 2005; 310:1139. [PubMed: 16293750]
- (14). Harbers, GM.; Grainger, DW. *Introduction to biomaterials*. Guelcher, SA.; Hollinger, JO., editors. CRC Press, Boca Raton, FL; Boca Raton: 2005. p. 15-45.
- (15). Engler AJ, Sen S, Sweeney HL, Discher DE. *Cell*. 2006; 126:677. [PubMed: 16923388]
- (16). Leipzig ND, Shoichet MS. *Biomaterials*. 2009; 30:6867. [PubMed: 19775749]
- (17). Banerjee A, Arha M, Choudhary S, Ashton RS, Bhatia SR, Schaffer DV, Kane RS. *Biomaterials*. 2009; 30:4695. [PubMed: 19539367]
- (18). Teixeira AI, Ilkhanizadeh S, Wigenius JA, Duckworth JK, Inganas O, Hermanson O. *Biomaterials*. 2009; 30:4567. [PubMed: 19500834]



- (19). Saha K, Keung AJ, Irwin EF, Li Y, Little L, Schaffer DV, Healy KE. *Biophys. J.* 2008; 95:4426. [PubMed: 18658232]
- (20). Seidlits SK, Khaing ZZ, Petersen RR, Nickel JD, Vanscoy JE, Shear JB, Schmidt CE. *Biomaterials.* 2010; 31:3930. [PubMed: 20171731]
- (21). Benoit DSW, Schwartz MP, Durney AR, Anseth KS. *Nat. Mater.* 2008; 7:816. [PubMed: 18724374]
- (22). Burdick JA, Anseth KS. *Biomaterials.* 2002; 23:4315. [PubMed: 12219821]
- (23). Lin C, Anseth KS. *Adv. Funct. Mater.* 2009; 19:2325. [PubMed: 20148198]
- (24). Schneider GB, English A, Abraham M, Zaharias R, Stanford C, Keller J. *Biomaterials.* 2004; 25:3023. [PubMed: 14967535]
- (25). Chen YM, Ogawa R, Kakugo A, Osada Y, Gong JP. *Soft Matter.* 2009; 5:1804.
- (26). Dadsetan M, Knight AM, Lu L, Windebank AJ, Yaszemski MJ. *Biomaterials.* 2009; 30:3874. [PubMed: 19427689]
- (27). Rao SS, Han N, Winter JO. *J. Biomater. Sci. Polymer Edn.* 2011; 22:611.
- (28). Hynes SR, McGregor LM, Rauch MF, Lavik EB. *J. Biomater. Sci. Polymer Edn.* 2007; 18:1017.
- (29). Wang J-H, Hung C-H, Young T-H. *Biomaterials.* 2006; 27:3441. [PubMed: 16516286]
- (30). Yavin E, Yavin ZJ. *Cell Biol.* 1974; 62:540.
- (31). Cai L, Wang S. *Biomacromolecules.* 2010; 11:304. [PubMed: 20000349]
- (32). Wang S, Lu L, Gruetzmacher JA, Currier BL, Yaszemski MJ. *Biomaterials.* 2006; 27:832. [PubMed: 16102819]
- (33). Kim S, English AE, Kihm KD. *Acta Biomater.* 2009; 5:144. [PubMed: 18774763]
- (34). Motala-Timol S, Jhurry D, Zhou J, Bhaw-Luximon A, Mohun G, Ritter H. *Macromolecules.* 2008; 41:5571.
- (35). Schmidt CE, Shastri VR, Vacanti JP, Langer R. *Proc. Natl. Acad. Sci. USA.* 1997; 94:8948. [PubMed: 9256415]
- (36). Kater SB, Mills LR. *J. Neurosci.* 1991; 17:891. [PubMed: 2010811]
- (37). Georges PC, Miller WJ, Meaney DF, Sawyer ES, Janmey PA. *Biophys. J.* 2006; 90:3012. [PubMed: 16461391]

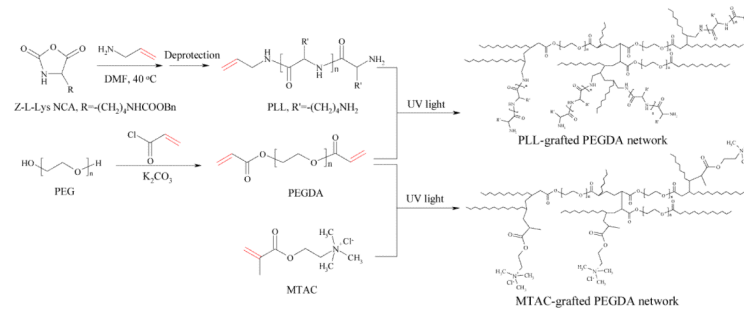


**Figure 1.** Synthesis of polymerizable PLL and PEGDA, and preparation of PEGDA networks grafted with PLL or MTAC via photo-crosslinking.

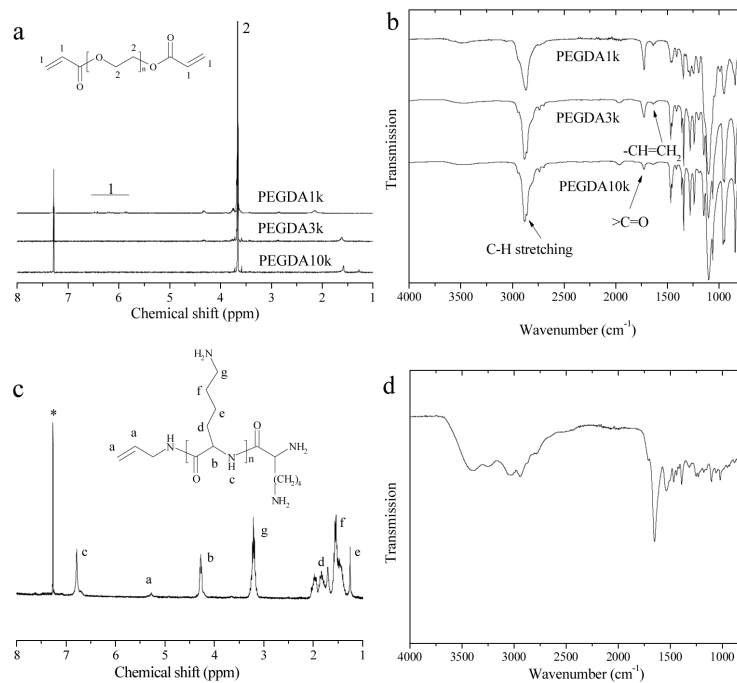


**Figure 2.** (a) NMR and (b) IR spectra of PEGDA1k, 3k, and 10k, (c) NMR and (d) IR spectra of photo-crosslinkable PLL. \*: CDCl<sub>3</sub> peak.

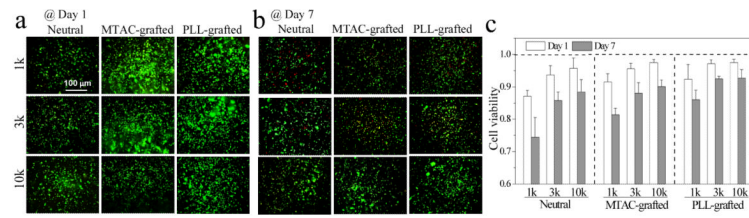


**Figure 3.**

PC12 cells encapsulated in neutral, MTAC-grafted, and PLL-grafted PEGDA hydrogels for (a) 1 and (b) 7 days. Scale bar of 100 μm is applicable to all. (c) Cell viability after encapsulation in the hydrogels for 1 and 7 days.  $p < 0.05$  between neutral and PLL-grafted hydrogels made from the same PEGDAs at day 7; between hydrogels made from PEGDA1k and 3k or 10k; between day 1 and day 7.

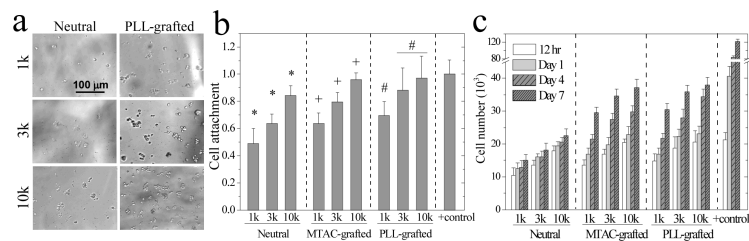


**Figure 4.** PC12 cell attachment and proliferation on the hydrogels. (a) Phase contrast images of PC12 cells cultured for 7 days. Scale bar of 100 μm is applicable to all. (b) PC12 cell attachment at 12 h post-seeding. \*:  $p < 0.05$  between two marked samples. +, #:  $p < 0.05$  between two marked samples and compared to the corresponding data on the neutral hydrogels. Positive (+) control: TCPS. (c) PC12 cell proliferation at 12 h, days 1, 4, and 7 post-seeding.  $p < 0.05$  between hydrogels made from the same PEGDAs at the same time, except for between PLL-grafted hydrogels of PEG3k and 10k at 12 h and day 1. Positive (+) control: TCPS.



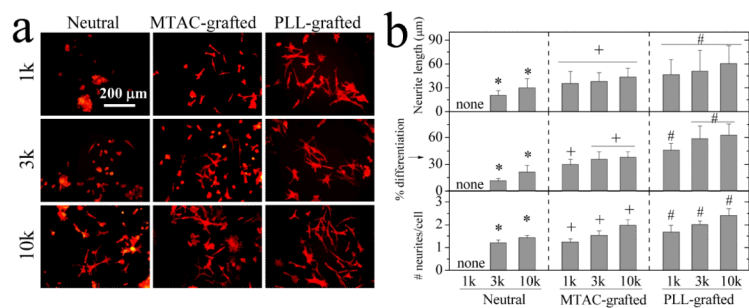


**Figure 5.**

PC12 cell differentiation on the hydrogels. (a) Fluorescent images of PC12 neurites induced by NGF at day 7. Stained with rhodamine-phalloidin. Scale bar of 200 μm is applicable to all. (b) Neurite length, percentage of differentiated cells, and the number of neurites per cell for PC12 cells at day 7. \*:  $p < 0.05$  between two marked samples. +, #:  $p < 0.05$  between two marked samples and relative to neutral hydrogels made from the same PEGDAs.

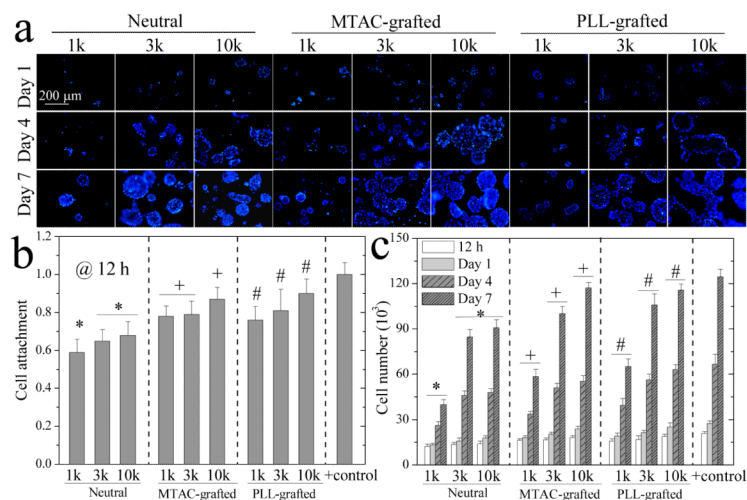


**Figure 6.** NPC proliferation on the hydrogels. (a) Nuclei (blue) of NPCs for 1, 4, and 7 days. Scale bar of 200  $\mu\text{m}$  is applicable to all. (b) NPC attachment at 12 h post-seeding. Positive (+) control: TCPS. (c) NPC cell number at 12 h, days 1, 4, and 7 post-seeding. \*:  $p < 0.05$  between two marked samples at the same time. +, #:  $p < 0.05$  between two marked samples and relative to the neutral hydrogels made from the same PEGDAs at the same time. Positive (+) control: TCPS.

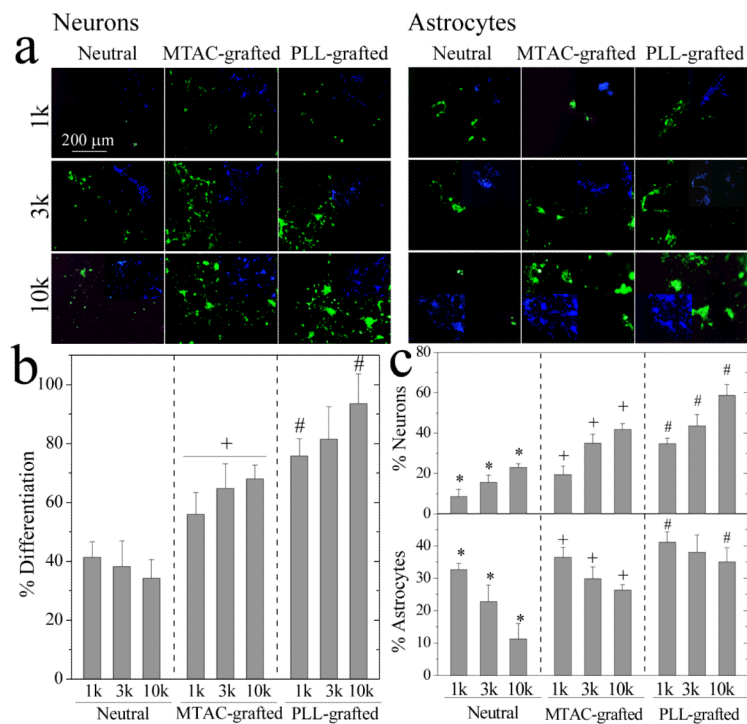


**Figure 7.** NPC differentiation on the hydrogels. (a) NPC differentiated neurons stained with anti- $\beta$ -tubulin-III (green, left side) and astrocytes stained with anti-GFAP (green, right side) at day 7. Inset is DAPI nuclear staining (blue) of the same field. Scale bar of 200  $\mu$ m is applicable to all. (b) Percentage of differentiated NPCs. +:  $p < 0.05$  relative to neutral and PLL-grafted hydrogels made from the same PEGDAs. #:  $p < 0.05$  between two marked samples. (c) Percentages of differentiated neurons and astrocytes. \*:  $p < 0.05$  between two marked samples. +, #:  $p < 0.05$  between two marked samples and relative to neutral hydrogels made from the same PEGDAs.

Table 1

Physical properties of the hydrogels.

PEGDA hydrogels	Swelling ratio	Gel fraction (%)	Shear modulus (kPa)	Zeta potential (mV)
Neutral				
1k	5.4 ± 0.5	77 ± 8	246 ± 7	0
3k	6.4 ± 0.1	73 ± 1	76.5 ± 0.3	0
10k	14.7 ± 1.0	68 ± 5	10.6 ± 0.5	0
MTAC-grafted				
1k	5.8 ± 0.3	78 ± 3	265 ± 12	8.8 ± 1.1
3k	7.6 ± 0.8	72 ± 4	72.8 ± 1.4	8.4 ± 0.6
10k	15.9 ± 0.7	67 ± 6	10.4 ± 0.4	7.4 ± 0.5
PLL-grafted				
1k	5.6 ± 0.6	78 ± 5	269 ± 5	5.0 ± 0.8
3k	6.9 ± 0.5	74 ± 5	75.9 ± 0.7	4.2 ± 0.2
10k	14.8 ± 0.6	70 ± 2	11.7 ± 1.1	4.1 ± 0.5